THE AMERICAN MINERALOGIST, VOL. 44, MAY–JUNE, 1959

A COMPARATIVE STUDY OF TEN MONAZITES

MARTIN W. MOLLOY, *Columbia University, New York, New York.*

ABSTRACT

Optical, *x*-ray, and differential thermal methods are used to compare monazite recently discovered near Chester, New Jersey, with monazite from nine other localities. Indices of refraction, 2V and birefringence have been determined. *X*-ray diffraction patterns have been measured, indexed, and their relationships determined. Micro-camera diffraction patterns have provided information on the alteration of monazite. The application of *x*-ray fluorescence to the quantitative analysis of rare earth elements in monazite is shown to be feasible through sensitivity to minor variations caused by crystal fractionation. Theoretical factors which interfere with precise *x*-ray fluorescence, quantitative analysis of rare earth elements in monazite are examined. The effect of two types of alteration, intercrystalline and intracrystalline, upon the differential thermal pattern of monazite is observed.

INTRODUCTION

Monazite was found near Chester, Morris County, north central New Jersey during the recent, intense search for uranium. A pit in the topsoil of Mr. William Waldon's cornfield provided the first specimens. The Mineralogical Laboratory of the Department of Geology, Columbia University, received radioactive samples from this locality from Eastern Uranium, Inc.

The specimens are dense, fine-grained, reddish brown, with surficial limonite staining, and are cut by coarsely crystalline, non-radioactive quartz veins. The radioactive material is monazite with a high thorium content. Partial chemical analysis by Ledoux and Company, Teaneck, New Jersey, reports 53.36 per cent total rare earth oxide, 13.66 per cent ThO_2, 25.31 per cent P_2O_5, and 0.045 per cent U_3O_8. In thin section the specimens show numerous, euhedral monazite crystals associated with zoned zircon and quartz (Pl. 1: 1*a*, 1*b*).

About 200 pounds of high-grade monazite were recovered from the property. The monazite occurs both as soil residium and fractured blocks, associated with fractured blocks of quartz-feldspar granite. A 20 foot deep trench failed to reveal bedrock.

Specimens from this locality have been studied over a two year period. During this time the Chester monazite has been compared with specimens from nine other localities utilizing optical, *x*-ray diffraction, *x*-ray fluorescence, and differential thermal methods. Material from Chester has also been examined by Drs. E. C. T. Chao and Charles Milton of the U. S. Geological Survey (Markewicz, Chao, and Milton, 1957).

This study has been materially aided by the cooperation of the New Jersey Department of Conservation and Economic Development. Dr. Meredith Johnson and Mr. Frank Markewicz have been particularly helpful in the interpretation of field relations.

This problem was suggested, and the study guided by Dr. Paul F. Kerr, Professor of Mineralogy, Department of Geology, Columbia University. Substantial assistance has been received in the interpretation of differential thermal data from Dr. Otto Kopp, and of x-ray diffraction data from Mr. Samuel Kamhi. To these and to Miss Peggy-Kay Hamilton, Dr. Dana Kelley, and Dr. William A. Bassett of the mineralogy group at Columbia the writer wishes to express his appreciation for their kind assistance.

Monazite Localities

The monazite localities listed below are referred to in the text that follows by the simplified locality names. In the tables the Chester occurrence is listed first, followed by other localities in alphabetical order. These specimens were large, single crystals without megascopic intergrowths of foreign material, and were obtained from the Mineralogical Research Collection of the Department of Geology, Columbia University.

Locality Information	*Locality Name*
William Waldon farm, Chester, Morris County, New Jersey	Chester
Amelia, Virginia, #234C Hoadley Collection, from the D'Agostino Collection	Amelia
"Cryptolite in Apatite," N'otero, Arendal, Norway	Arendal
Augusta Court House, Virginia, Eggleston Collection	Augusta
Madison County, North Carolina; G. L. English and Company, New York	Madison
Minas Geraes, Brazil	Minas Geraes
Missoula, Montana	Missoula
South Lynne, Connecticut (Matthews, 1894)	S. Lynne
Ramsey Mine, Toledo, North Carolina	Toledo
Ural Mountains, Russia	Urals

Optical Properties

Oriented and random thin sections, as well as fragment mounts, were studied with the petrographic microscope and universal stage. Indices of refraction were determined in sodium light with high index liquids (Meyrowitz and Larsen, 1951). The optical properties are given in Table 1.

The extent of alteration is indicated by the color of the mineral, which changes from greenish yellow to opaque brown as alteration increases. Cleavage and alteration are also related. Unaltered specimens are free from cleavage, but as alteration increases, cleavage appears first in one, then in two, and finally in three directions. The most altered specimens have the lowest indices of refraction, while the least altered specimens yield the highest indices.

The associated alteration consists of limonite-stained masses or cloud-

TABLE 1. OPTICAL PROPERTIES OF TEN MONAZITES

Locality	Color	Cleavage Directions	Refractive Index (±.002) n_α	n_γ	Birefringence	2V+	Degree of Opacity (Associated Alteration in per cent)
Chester	Yellow-brown	1 Good 1 Poor	1.775	1.836	.061	16°	75
Amelia	Greenish-yellow	Indistinct	1.788	1.851	.063	13°	25
Arendal	Greenish-brownish-yellow	Indistinct	1.780	1.839	.059	11.5°	37
Augusta	Greenish-yellow	Indistinct	1.774	1.849	.075	15°	65
Madison	Greenish-yellow	None	1.782	1.850	.068	16°	15
Minas Geraes	Brownish-greenish-yellow	2 Poor	1.790	1.850	.061	13°	50
Missoula	Greenish-brownish-yellow	Indistinct	1.789	1.847	.058	12°	30
S. Lynne	Greenish-brown	2 Poor	1.777	1.841	.064	15°	70
Toledo	Brown	2 Good	1.775	1.828	.053	15°	63
Urals	Brown	3 Good	1.784	1.843	.059	16°	63

like clusters of minute, opaque particles which spread through monazite crystals, sometimes following cleavage planes (Pl. 2: 2*a*, 2*b*). The degree of opacity is a measure of the degree of alteration and was determined by PhotoVolt meter readings on representative areas of oriented thin sections.

In thin section monazite is not noticeably pleochroic. The dispersion $r<v$ is weak. All specimens were biaxial positive with a small 2V. The optic angle does not show a clear relation either to the degree of associated alteration or to the chemical composition as indicated by *x*-ray fluorescence. The only example of twinning was found in the Toledo specimen, and this was of the polysynthetic type. The Madison sample consisted of rounded, placer grains, and except for this and the previously described Chester material, all specimens were large, single crystals.

DIFFERENTIAL THERMAL ANALYSIS

The monazite specimens were examined by differential thermal analysis using equipment previously described (Kerr and Kulp, 1948; Kulp and Kerr, 1949; Kulp and Perfetti, 1950). Background drift effects were removed and the corrected curves plotted (Fig. 1). In all cases sample grain size and furnace loading were duplicated as closely as possible. Despite attempts at standardization, minor variations may occur in thermal patterns produced by the same material in different furnace

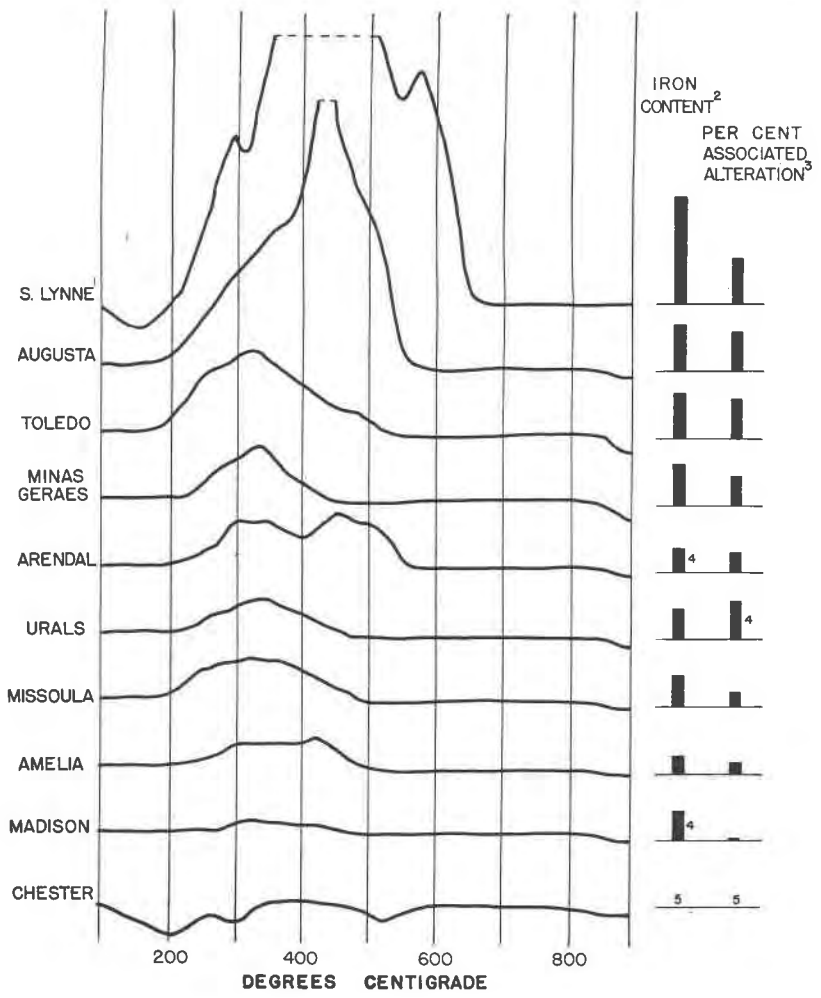

FIG. 1. Differential thermal curves of ten monazites[1] in comparison with iron content[2] and per cent alterations.[3]

[1] Arranged in order of the intensity of the 330° C. peak.

[2] From *x*-ray fluorescence analysis.

[3] Determined by PhotoVolt light meter readings on representative areas of oriented thin sections.

[4] Order inconsistent with that of thermal peaks.

[5] Interstitial limonite masks pattern from intracrystalline alteration.

runs; however, no significant variations in peak position or intensity were observed.

The exothermic reactions recorded occur in the 200–600° C. range. The

TABLE 2. *d* Å AND RELATIVE INTENSITY DIFFRACTION PATTERNS OF TEN MONAZITES

Chester		Amelia		Arendal		Augusta		Madison		Minas Geraes		Missoula		S. Lynne		Toledo		Urals	
														5.40	10				
5.23	10	5.26	16			5.25	11	5.21	12	5.22	10	5.22	6	5.21	13	5.21	17	5.22	10
5.17	10			5.17	9											5.16	14	5.16B	9
						5.05	9												
4.82	8	4.82	8							4.80	12	4.81	15			4.78	22	4.81	12
4.68	17	4.69	14	4.68	13	4.67	17	4.68	7	4.68	13	4.68	16	4.68	16	4.67	35	4.68	19
														4.42	13				
4.18	37	4.18	25	4.17	23	4.18	22	4.17	19	4.19	23	4.17	21	4.18	36	4.17	40	4.18	28
4.10	29	4.10	18	4.09B	14	4.10	11			4.10	19	4.11	18	4.11	19	4.08	23	4.10	19
3.95	10							3.95	8										
						3.85	11			3.85	9	3.84	7						
														3.53	23	3.54	27	3.53	18
3.52	29	3.52	25	3.51	44	3.49	19	3.51	44	3.51	32	3.51	28	3.51	33	3.52	31	3.51	29
3.44	15	3.48	14							3.46	13	3.46	6			3.44	48		
3.30	71	3.29	44	3.28	73	3.28	53	3.29	63	3.30	61	3.29	75	3.30	87	3.29	85	3.30	90
3.21B	11							3.21B	12			3.21	7						
						3.12	11							3.13	11	3.13	20	3.13	36
3.09	100	3.08	100	3.07	100	3.07	100	3.08	100	3.08	100	3.08	100	3.08	100	3.08	100	3.09	100
2.98	25	2.98	16	2.97	17	2.98	20	2.98	12	2.98	13	2.98	19	2.99	17	2.98	25	2.98	13
		2.96	12																
2.87	53	2.88	46	2.87	39	2.88	31	2.87	40	2.88	22	2.88	28	2.87	49	2.87	96	2.87	59
2.83	22					2.81	5					2.91	6	2.83	11				
2.79	8	2.78	7											2.79	9	2.79	17	2.78	7
2.70B	6	2.70	6	2.71B	5			2.71	7	2.71	9			2.72	7	2.72	11		
						2.67	5			2.65	6			2.65	13	2.68	7	2.68	7
2.61	19	2.62B	8	2.61B	6	2.61	12	2.61B	9	2.62B	12	2.60	10	2.61	23	2.61	15	2.61	16
2.57	5	2.57B	6	2.58	8					2.58B	5	2.58B	5						
		2.52	5	2.52	5														
2.45B	19	2.45	16	2.44B	6	2.45B	11	2.43	14	2.44	14	2.44	18	2.44	26	2.44	23	2.44	12
2.41	7			2.41	6			2.40	8			2.40	12			2.41	17		
						2.29	9												
2.21	19	2.22B	9																
2.17B	24	2.17	16	2.16	14	2.16	20	2.17	39	2.17	28	2.18	15	2.17	23	2.18	27	2.17	14
2.13	36	2.13B	21	2.13	14	2.13B	19	2.13	16	2.14	23	2.13	15	2.13	29	2.13	35	2.13	25

Chester		Amelia		Arendal		Augusta		Madison		Minas Geraes		Missoula		S. Lynne		Toledo		Urals	
2.12	39	2.12B	23	2.11B	16	2.11B	20	2.11	18	2.11	19	2.12B	18	2.11	37	2.11	27	2.11	20
2.09	24							2.09	11			2.09	6						
2.08	27							2.07	11										
2.03	15					2.02	8												
1.99	15									1.99	7								
1.98	17	1.98	25			1.98	8			1.98B	10	1.98B	13	1.98	27	1.98	25	1.98	20
1.97	14			1.97B	14			1.97B	16							1.97	12		
1.94	14			1.95	10					1.95B	10	1.95	11	1.95	14	1.95	9		
1.90B	17	1.90	14			1.90	5	1.92	10	1.91	13			1.90	13	1.91	15	1.90	12
1.88B	15	1.88	39	1.88B	13	1.88B	16			1.88B	13	1.88	21	1.88	24	1.88B	17	1.88B	20
				1.87B	16	1.87B	17	1.87B	21	1.87	26	1.86	21	1.86	27	1.85	17		
1.79	14	1.80	10	1.79	12			1.81	12							1.79	15	1.79B	10
1.78	10					1.78	12												
1.77	10	1.77	7									1.77	10	1.77	20	1.77	7		
		1.75B	14	1.75B	12					1.76	12					1.75	21	1.75B	13
1.73	20	1.73	16			1.73B	14	1.73	26	1.73	19	1.73	19	1.73	19	1.73	27		
1.72	20			1.72B	13	1.72B	13							1.72	19	1.72B	20	1.72	14
		1.69	18	1.69	11	1.69	17	1.69B	19	1.69B	14	1.69	16	1.69B	11	1.69	15	1.69	14
1.65	17	1.65	14	1.66	8	1.65	11	1.65	8	1.65B	7			1.65	11	1.65	12		
		1.62	9																
1.61	17	1.61	11			1.61	8	1.61	6	1.61	14	1.61	7	1.61	11				
1.59	15			1.59	7			1.59	5					1.59	10	1.58	13	1.59	16
1.54	12	1.55B	7							1.55	9					1.57	10		
																		1.53	6

B = broad.

broad, moderately intense peak is a composite of three exothermic reactions, which are distinctly resolved in the S. Lynne pattern. These occur about 250° C., 330° C., and 430° C. with the last peak being delayed until 570° C. in specimens with intense reactions. This indicates that the high temperature peak is due to oxidation, and is delayed by depletion of oxygen in the system by a previous oxidation reaction.

The Chester sample shows endothermic reactions at 250–300° C. and 560° C. The lower peak is distorted by the effects of the superposed 250° C. and 330° C. exothermic reactions noted above. A similar exothermic trend appears at the start of the S. Lynne pattern. The bifurcation noted in the high temperature exothermic peak of the Arendal material has not been explained.

Evaluation of the Differential Thermal Analysis

As a common placer mineral, monazite is distinguished by chemical resistance and refractivity. Madison, the sample showing the least alteration, has an almost featureless differential thermal pattern, while S. Lynne and Augusta, samples with high iron content and extensive alteration, yield pronounced exothermic reactions. The relation of iron content, degree of alteration, and intensity of the exothermic reactions is shown in each sample by the height of the 330° C. peak (Fig. 1). It seems likely that the exothermic reactions recorded are due to alteration and iron content, and that the differential thermal pattern of an alteration- and iron-free monazite would be featureless.

The alteration in the Chester monazite is predominately intercrystalline, as opposed to the almost exclusively intracrystalline nature of the alteration in the other monazites. While the monazite crystals of the Chester sample are only slightly altered, they are surrounded by large areas of reddish brown, isotropic material (Pl. 1: 1*a*, 1*b*). *X*-ray diffraction micro-camera photographs show this material to be primarily goethite. The differential thermal pattern of goethite is distinguished by a single, large endothermic reaction in the 300–400° C. region (Posnjack and Merwin, 1919). Poorly crystalline goethite gives the same reaction at 293° C. or lower (Arens, 1951). The alteration in the Chester sample yields water when heated. The effect of the endothermic reactions of goethite and water upon the exothermic pattern of monazite would be a distortion of both patterns. The Chester pattern is therefore interpreted as a composite of the 250° C., 330° C., and 430° C. exothermic reactions due to the monazite alteration superimposed on the 200–400° C. endothermic reactions of goethite and water.

Differential thermal analysis indicates that the thermal pattern of unaltered monazite is featureless, and that the reactions observed are

caused by the oxidation and inversion of iron present in the alteration minerals. The associated 250° C., 330° C., and 430° C. exothermic alteration reactions are sufficiently consistent, however, to suggest the presence of monazite in differential thermal curves.

X-Ray Diffraction

Except for a similarity to huttonite (Pabst and Hutton, 1951), monazite is easily distinguished by its characteristic *x*-ray powder pattern. Variation in rare earth composition causes a small range in cell dimensions among different monazites. Lines caused by significant, crystalline impurities often appear superimposed on a monazite pattern.

In the 2θ range, 10–60°, 93 reflections may be computed for monazite. This complex structure plus the variety of substitutions possible among its rare earth and thorium components, creates an intricate diffraction pattern with a few intense reflections and many that are small and overlap. In such a case the impulse counting technique of the *x*-ray diffractometer has been used in preference to the photographic method for the detection of faint reflections and in determining relative intensities.

Diffractometer charts produced by the Norelco instrument have been analyzed, and a tabulation of *d* Å spacings and relative intensity measurements prepared (Table 2). These data have been plotted graphically in Fig. 2 to show the range in intensity and position of the monazite reflections. In this plot, the data from Fig. 1 are represented as points, and vertical lines have been drawn joining points with the same (*hkl*) value. The accuracy of these *d* Å measurements increases as the spacing decreases, with the error diminishing from ± 0.05 Å for the largest spacing to ± 0.002 Å for the smallest.

The unit cell dimensions for monazite by Gliszczynski (1939) and Parrish (1939) are listed in Table 3. These yield the theoretical *d* Å spacings corresponding to the (*hkl*) values of monazite when substituted in the indexing equation for a monoclinic crystal (Klug and Alexander, 1954).

Table 3. Unit Cell Dimensions of Monazite

	Gliszczynski	Parrish
a_0	6.782 kX	6.76 kX
b_0	6.993 kX	7.00 kX
c_0	6.445 kX	6.42 kX
β	76°22′	76°50′
$a:b:c$	.9686:1:.9231	.9660:1:.9167
S.G. (meas.)	—	5.173
S.G. (calc.)	5.217	5.06
Cell Volume	—	296

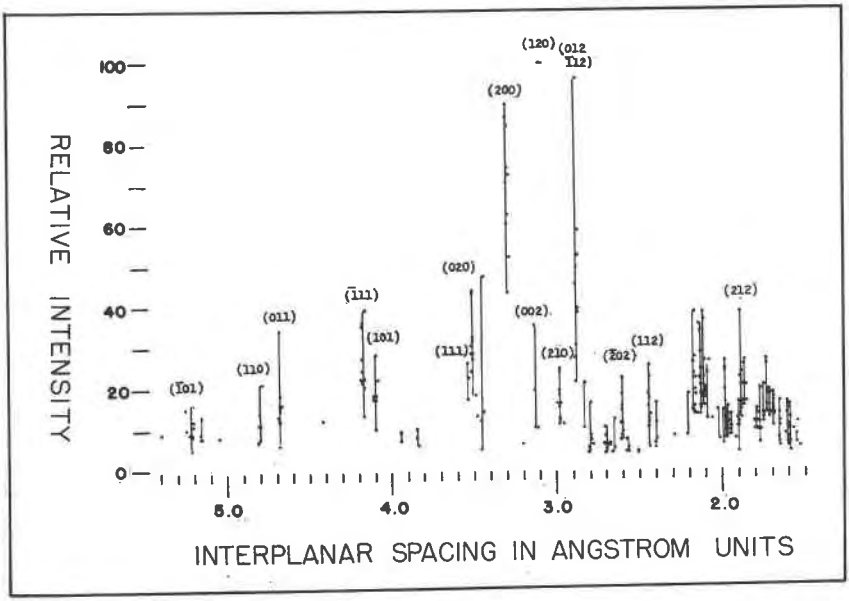

FIG. 2. Relative intensity vs d Å for monazite. Both the range in reflection position and intensity for any lattice plane are indicated in this diagram.

The calculations are listed in Table 4 in comparison with the ASTM monazite standard (Chochi-wan, Southern Korea; Pabst and Hutton, 1951), and the spacings obtained from the ten monazites studied (Table 2). Spacings which do not correspond to theoretical values are listed separately and are attributed to crystalline impurities. A number of spacings in the small d Å range may coincide with reflections caused by impurities.

THE ALTERATION OF MONAZITE

The nature of the alteration of monazite is of interest. X-ray diffraction patterns show reflections unaccounted for by the monazite structure (Table 4). However, the diffraction pattern of monazite masks that of goethite and other expectable minerals. Unless the fine alteration constituents can be concentrated to yield a pattern distinct from the host mineral, the powder method has serious limitations for identification.

It is possible to study randomly oriented crystallites as small as 50 microns (0.002 inches) in diameter, and obtain a diffraction photograph with the x-ray micro-camera. The technique was developed for use in synthetic fiber studies by Fankuchen and Mark (1944), and subsequently applied to mineral identification in the clay alteration studies of Kelley and Kerr (1957).

TABLE 4. *X*-RAY DIFFRACTION SPACINGS OF TEN MONAZITES FOR THE RANGE d Å $= \infty - 1.530$

hkl	$d_{calc.}$ (Å)*	Reference Monazite†		Ten Monazites $d_{obs.}$ (Å)	Impurities d Å
		d Å	I/I		
					5.40
$\bar{1}01$	5.205	5.23	40	5.21–5.26	5.16–5.18
110	4.806	4.72	40	4.78–4.82	4.05
011	4.677			4.67–4.69	4.42
$\bar{1}11$	4.178	4.17	60	4.17–4.19	3.95
101	4.090			4.08–4.11	3.84–3.85
111	3.537	3.52	50	3.53–3.54	3.48
020	3.504			3.49–3.52	3.44–3.46
200	3.299	3.31	70	3.28–3.30	3.21
002	3.143			3.12–3.13	
120	3.095	3.09	100	3.07–3.09	
021	3.060				
210	2.988	2.99	20	2.97–2.99	
$\bar{2}11$	2.953				
$\bar{1}21$	2.908				
012	2.867	2.88	70	2.87–2.88	2.81
$\bar{1}12$	2.865				
221	2.835			2.83	2.78–2.79
121	2.662			2.65–2.68	2.70–2.72
$\bar{2}02$	2.604	2.61	20	2.60–2.62	2.57–2.58
211	2.495				2.52
112	2.447	2.45‡	30B	2.43–2.45	
$\bar{2}12$	2.441			2.40–2.41	
220	2.403				
022	2.340				
$\bar{1}22$	2.338				
$\bar{3}01$	2.251				2.29
130	2.202				2.21–2.22
013	2.189	2.19	40	2.16–2.18	
$\bar{1}03$	2.148				
$\bar{3}11$	2.142	2.14	60	2.13–2.14	
131	2.131				
221	2.126			2.11–2.12	
310	2.100				
$\bar{1}22$	2.093				
$\bar{2}22$	2.090			2.09	2.07–2.08
$\bar{1}13$	2.054				
202	2.048				
131	2.029			2.02–2.03	
013	2.007				
$\bar{2}03$	1.995			1.98	
212	1.967	1.97	50	1.97	
$\bar{3}12$	1.962	1.96	10		
301	1.941			1.94–1.95	
$\bar{2}13$	1.919			1.90–1.91	
230	1.907	1.90B	20		
$\bar{2}31$	1.898				

B = broad.

* Calculations based on the unit cell dimensions of Gliszczynski (1939), see Table 3. Systematic extinction occurs when $k \neq 2n$ in $0k0$, and $h+l \neq 2n$ in $h0l$. In addition, $\bar{h}\bar{k}\bar{l} = hkl$; $hkl = h\bar{k}l$; and $\bar{h}kl = hk\bar{l}$.

† ASTM reference monazite, Pabst and Hutton (1951).

‡ Spacings on the ASTM card were not indexed beyond this point.

TABLE 4 (*continued*)

hkl	$d_{calc.}$ (Å)*	Reference Monazite†		Ten Monazites $d_{obs.}$ (Å)	Impurities *d* Å
		d Å	I/I		
$\bar{3}21$	1.893	1.88B	60	1.88–1.89	
032	1.875				
103	1.874			1.85–1.87	
$\bar{1}32$	1.874				
311	1.866				
320	1.864				
113	1.817			1.79–1.81	
$\bar{1}23$	1.817				
023	1.798	1.80	20		
222	1.769	1.77	40	1.77	1.78
$\bar{3}22$	1.766				
231	1.760			1.75–1.76	
040	1.752	1.75	60		
132	1.741				
$\bar{2}32$	1.739				
$\bar{3}03$	1.735				
223	1.733			1.73	1.72
321	1.697	1.70	60	1.69	
140	1.693				
$\bar{0}41$	1.687				
313	1.687				
$\bar{4}02$	1.662				
$\bar{1}41$	1.660			1.65–1.66	
123	1.657				
400	1.651	1.65	10		
$\bar{4}11$	1.650				
$\bar{3}31$	1.620	1.63	10	1.62	
$\bar{4}12$	1.618				
$\bar{1}04$	1.617				
$\bar{2}04$	1.615				
141	1.611	1.61	10	1.61	
410	1.607				
330	1.602				
312	1.589			1.58–1.59	
$\bar{1}14$	1.575				
$\bar{2}14$	1.574				
004	1.571			1.57	
213	1.565				
033	1.559				
$\bar{3}23$	1.555				
240	1.548			1.54–1.55	
241	1.543				
232	1.540	1.54	40		
$\bar{3}32$	1.537				
014	1.533			1.53	
042	1.530				
$\bar{1}42$	1.530				

Minute, reddish brown masses comprising the opaque areas between monazite crystals in the Chester monazite (Pl. 1: 1*a*, 1*b*) were removed from the thin section and photographed with the micro-camera using molybdenum filtered iron radiation to reduce the intense background. The film obtained matched that of goethite, although there were extrane-

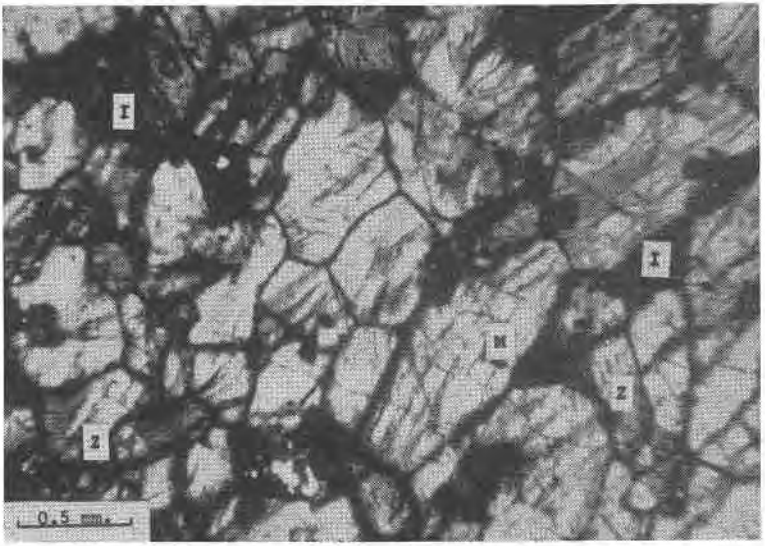

(a)

(b)

PLATE 1. a. Thin section, Chester; slightly altered, euhedral monazite crystals (M) associated with zoned zircon (Z) and interstitial iron oxides (I).

b. Thin section, Chester; embayed, zoned zircon crystal partly surrounded by iron oxides (I). (× nicols.)

(a)

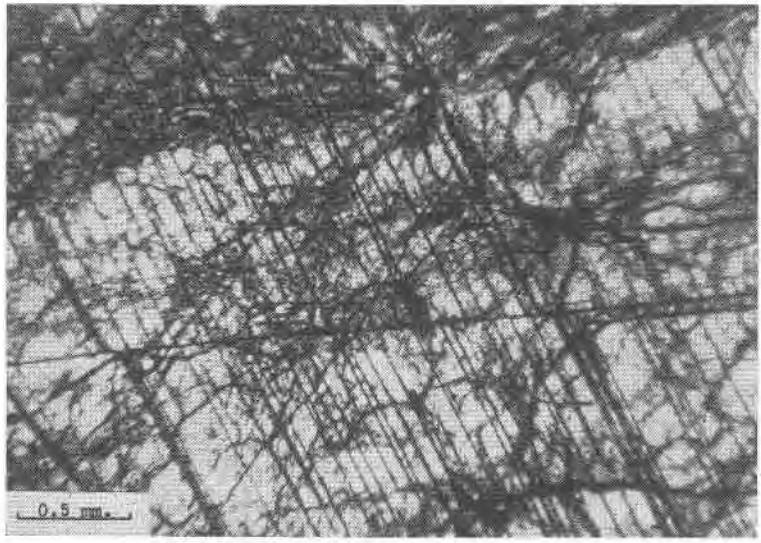

(b)

PLATE 2. a. Thin section, Minas Geraes; cloud-like alteration penetrating a single, uncleaved monazite crystal.

b. Thin section, Urals; alteration occurring both in patches and following the distinctive cleavage in this monazite crystal.

ous lines which could not be identified. Together with the high iron content from x-ray fluorescence and the nature of the thermal pattern, the micro-camera photographs confirm the identification of the opaque, interstitial material associated with the Chester sample as "limonite," or more specifically, goethite plus hydrous iron oxides (Mackenzie, 1957; Kulp and Trites, 1951; Blanchard, 1944).

However, limonite is not the alteration product within the monazite crystals. Thermal data indicate this to be a non-hydrous, ferrous oxide. Micro-camera photographs taken of areas of alteration in thin sections of the most altered specimens did not show any lines. Increasing the exposure of these photographs to 24 hours of Mn filtered Fe radiation produced no indication of a powder pattern due to the alteration mineral. With an exposure of this long a duration the white background continuum present even in filtered x-radiation is sufficient to produce a Laue photograph from the enclosing monazite crystal.

In view of the absence of any indication of crystallinity of the alteration product in the micro-camera photographs in specimens with a sufficient number of alteration particles to produce an x-ray diffraction pattern, the conclusion must be drawn that the material is not crystalline.

X-Ray Fluorescence Analysis

The elements from atomic number 57 to 71 (La, Ce, Pr, Nd, Sm, Eu, Gd, Tb, Dy, Ho, Er, Tm, Yb, and Lu) comprise the rare earth group. Accurate quantitative analysis for many of these elements is not possible by standard wet chemical methods. Such analysis is presently accomplished by emission spectroscopy and spectrophotometry. It is the purpose of this section to provide a basis for the extension of the x-ray fluorescence method (x-ray spectroscopy) to the quantitative analysis of rare earth elements in monazite.

X-ray spectroscopy is applicable to the detection of lithium (atomic number 3) and all heavier elements. The significant advantages of the fluorescence method are the reliability of the identification regardless of the particular element(s) involved, and the rapidity with which the analysis is made. Thus, in the case of the qualitative analysis of a complex system such as the rare earth elements in monazite, the x-ray fluorescence method is desirable.

The application of this method to the quantitative analysis of many of the common elements has already been done. This is dependent upon the fact that the intensity of the secondary x-ray spectra which an element may emit is a function of the amount of that element present in the sample. Measurement of the intensity of the secondary spectra of an

element, therefore, is the means by which quantitative analysis is accomplished by x-ray fluorescence.

When it is desirable to perform the quantitative analysis of an element by x-ray fluorescence, the particular instrument must be calibrated for that element. Normally this entails preparing a series of artificial standards closely approaching the sample in composition and covering the entire range of per cent in which the element is present. Often another element not found in the sample is added so that it will reflect any unusual events which may happen. This is known as the "internal standard" method. The samples are then run on the instrument and working curves for the elements prepared.

In the case of simple systems comprised of a few common elements, such procedure is routine. As the number of elements increases, however, the problem of mutual interference in their determination becomes most serious. The mineral monazite presents just such a case.

One of the major problems in dealing with the rare earth elements is the difficulty and expense in obtaining chemically pure material for the preparation of artificial standards. The other problem is the tendency of the rare earths to occur in groups rather than alone.

Eight rare earth elements (La, Ce, Pr, Nd, Sm, Gd, Dy, and Ho) in monazite are easily detectable by x-ray fluorescence. Several other elements (Th, Y, U, Pb, and Fe) accompany the rare earths. The x-ray tube background of W, Fe, Cu, and Ni should not be overlooked. Mutual interferences between these 17 elements form the barrier to the quantitative analysis of monazite by x-ray fluorescence. To eliminate this obstacle, the following analysis of these interferences was undertaken.

As has been pointed out, quantitative analysis of an element by x-ray fluorescence depends solely upon measurement of the intensity of the secondary spectra. Any factors which affect this intensity are known as interferences, and unless taken into account will markedly decrease the accuracy of the method. To emit a secondary spectra, an element must absorb energy, which, like the emission, occurs at specific wave lengths characteristic of that element. The interferences which occur may be summarized in terms of emission and absorption interactions of the following types: Emission Absorption, Emission Enhancement, and Competitive Absorption (Fig. 3).

In Emission Absorption, the intensity of a wave length emitted by one element is decreased due to the selective absorption of that wave length by another element present in the sample. A familiar example of this interference is the use of one element to filter the radiation produced by another.

Emission Enhancement of two types occurs. Spectra may overlap causing the intensity of one line to be increased by the proximity or

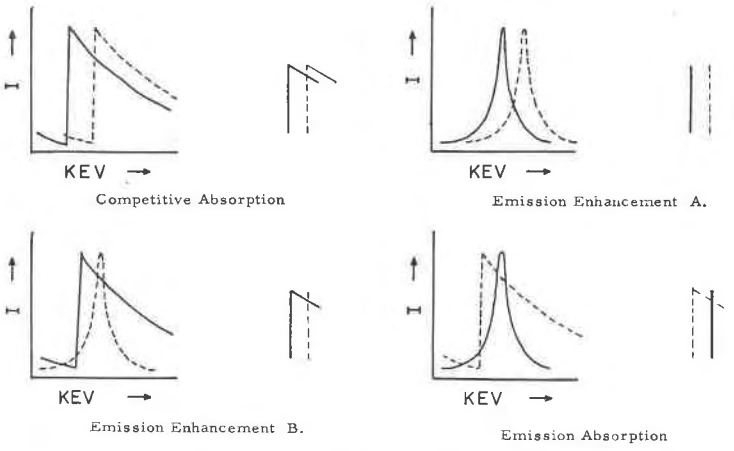

FIG. 3. Diagrammatic representation of the four types of phenomena which interfere with peak intensity in x-ray fluorescence analysis.

superposition of other lines. A similar increase in line intensity may be due to the absorption of energy by one element in the range in which another is emitting. Both these difficulties are commonly encountered in rare earth analysis.

With insufficient excitation potential, a decrease in emission intensity may be noted if two or more elements absorb energy in the same range. Interference of this nature is called Competitive Absorption and may be compensated for by the use of adequate excitation potential.

The emissions and absorptions of the 17 elements detected in the fluorescence analysis of monazite are listed in Table 5. The emissions which are the most useful for quantitative work and their absorption edges are shown as solid lines in Fig. 4. All other emissions and absorptions interfere with these and are plotted as dashed lines. The interferences shown in Fig. 4 are to be interpreted in terms of the four types given in Fig. 3. Fig. 4 provides the key for evaluating the nature of the interferences encountered in the analysis of the rare earth elements in monazite. The calibration of fluorescence equipment for the quantitative determination of any or all of the 17 elements shown may be accomplished by using Fig. 4 to determine the elements which interfere (dashed lines) with the emission line and absorption edge of the selected element (solid lines). Standard mixtures of the selected element with the interfering elements may then be prepared. The data obtained from these standards on the fluorescence equipment will provide the peak height or counts per second data from which working curves for the element may be prepared. Once the instrument has been calibrated, quantitative determination of the selected element is readily achieved.

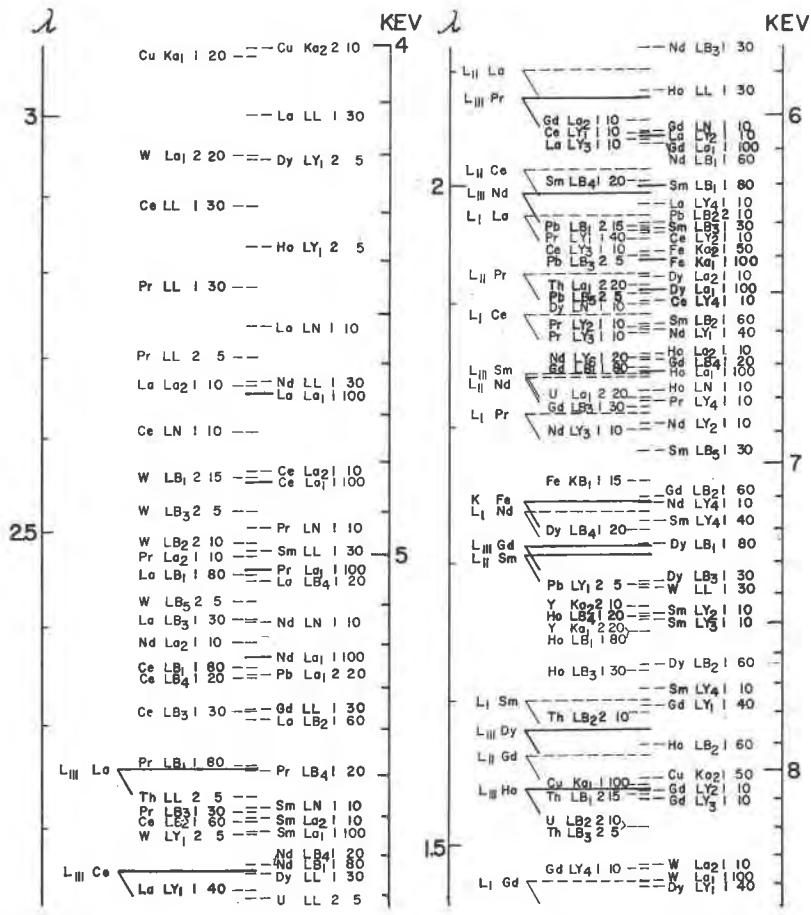

FIG. 4. Diagrammatic representation of emission lines and absorption edges (dashed lines) which interfere with accurate, quantitative analysis of the rare earth elements in monazite (solid lines).[1]

Both sample and tube background elements have been plotted. The notation used is the following: $L_{III}Ce$ represents the III absorption edge of the L series of cerium, while Ho LB_2 1 60 stands for the beta 2 emission of the first order of the L series of holmium which has a relative intensity[2] of 60 with respect to the L alpha 1 line of that element.

1. Prepared from the tables of Fine and Hendee (1954), and Powers (1957) using the conversion equation:

$$E(KEV) = \frac{12.39644 \pm .00017}{\lambda\ \text{Å}}$$

2. Lines with relative intensity less than 5 are not represented, and the intensities of lines of orders higher than 1 have been converted from the values of Power (1957)

(*Figure and legend are continued on next page*)

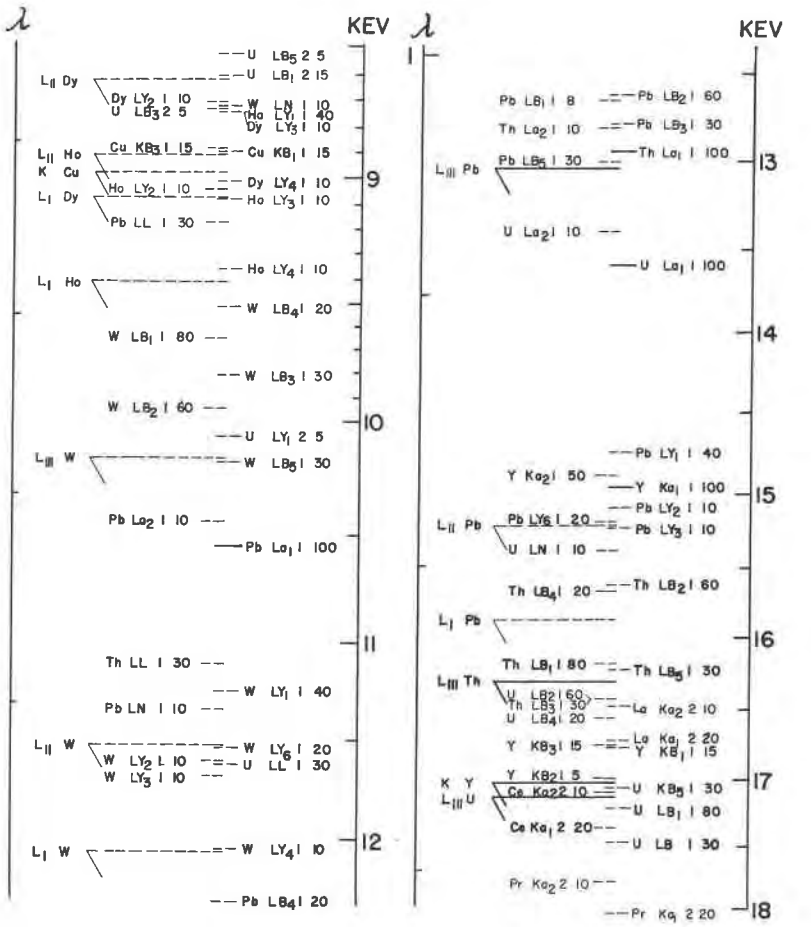

so that the intensities of all the lines of an element are directly comparable regardless of their order. For this conversion a high order line was assumed to be 1/20 the intensity of the same line in the next lowest order, and so reduced to the first order intensity. This assumption is valid for the LiF analyzing crystal which is widely used for this type of fluorescence analysis.

In the past, several workers have attempted such analysis without examining the interference problem. This is the primary limitation upon the usefulness of their work.

Goldschmidt and Thomassen (1924) were the first to attempt the quantitative analysis of the rare earths in monazite by *x*-ray spectroscopy. As was the custom of their time, the sample was made the target of the electron beam in a cathode ray tube. The primary radiation which

TABLE 5. QUANTUM MECHANICS TRANSITION RELATIONS FOR RARE EARTH *X*-RAY ENERGIES*

Emission Energies		Absorption Edges
Ka_1	=	K_{ab}–L_{III}
Ka_2	=	K_{ab}–L_{II}
Kb_1	=	K_{ab}–M_{III}
Kb_2	=	K_{ab}–N_{III}
La_1	=	L_{III}–M_V
La_2	=	L_{III}–M_{IV}
Lb_1	=	L_{II} –M_{IV}
Lb_2	=	L_{III}–M_V
$L\gamma_1$	=	L_{II} –M_{IV}

Therefore, the following absorption edges affect the corresponding emission energies of elements found in the monazite samples.

Emission Energies		Absorption Edges
La(La_1)	–	La(L_{III})
Ce(La_1)	–	Ce(L_{III})
Pr(La_1)	–	Pr(L_{III})
Nd(La_1)	–	Nd(L_{III})
Gd(La_1)	–	Gd(L_{III})
Sm(Lb_1)	–	Sm(L_{II})
Fe(Ka)	–	Fe(K_{ab})
Dy(La_1)	–	Dy(L_{III})
Ho(La_1)	–	Ho(L_{III})
Pb(La_1)	–	Pb(L_{III})
Th(La_1)	–	Th(L_{III})
U(La_1)	–	U(L_{III})
Y(Ka)	–	Y(K_{ab})

* From Fine and Hendee (1954).

it emitted was recorded on film and the line intensities determined with a photometer.

The difficulties of sample melting, segregation, volatilization, and the errors which these introduced were noted by von Hevesy (1932), and led to the abandonment of this type of analysis. In its place was employed analysis of the secondary, fluorescent *x*-radiation emitted by a sample bathed in the primary continuum from a tungsten target. The increased accuracy in angular measurement, the use of other types of radiation detectors (Parrish, 1956; Parrish and Kohler, 1956), and the recent development of the discrimination technique of Pulse Height Analysis using a proportional counter (Dowling, Hendee, Kohler, and Parrish, 1956; Miller, 1956), have provided reliable instrumentation to eliminate these errors.

Empirical investigation of the rare earth elements has been undertaken

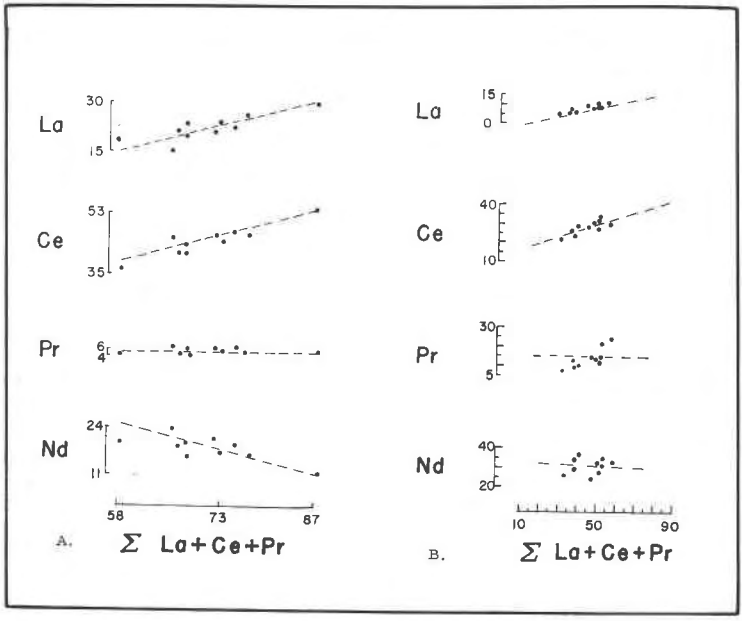

FIG. 5. Relation of the accuracy of the x-ray fluorescence method for determining rare earths in monazite to the emission spectrographic method (Murata, Rose, and Carron, 1953).

A. Atomic per cent (after Murata, Rose, and Carron, 1953). Plot of atomic percentages of rare earth elements (ordinate) versus the percentage of lanthanum group (abscissa). Dashed lines were calculated on the basis of fractional precipitation.

B. Uncorrected intensities from x-ray fluorescence. Plot of x-ray peak height (uncorrected) for rare earth elements (ordinate) versus the sum of the peak heights of the lanthanum group (abscissa). Dashed lines indicate trend of fractional precipitation.

by Dunn (1955), and Salmon and Blackledge (1955). It remains to unite such empirical work with the theoretical analysis in this paper.

While the mutual interferences preclude precise quantitative analysis at this time, in the case of several of the rare earth elements a semi-quantitative analysis is possible. This may be seen in Fig. 5 where the uncorrected peak heights from the x-ray fluorescence of the ten monazites (Table 6) have been plotted following the rules for the systematic variation of rare earths in monazite (Murata, Rose, and Carron, 1953). In the case of lanthanum and erbium the plots follow the trends they predict. On this basis, the peak heights listed in Table 6 may be used as a semi-quantitative means for comparing the rare earth content of the ten monazites. In the case of thorium, chemical analysis of the Chester monazite has shown that the recorded La_1 Th peak height of 74.5 corresponds to 13.66 per cent ThO_2. The complexity of this problem of

TABLE 6. *X*-RAY FLUORESCENCE PEAK INTENSITIES FOR TEN MONAZITES*

	Peak Intensity above Background												
	La($L\alpha_1$)	Ce($L\alpha_1$)	Pr($L\alpha_1$)	Nd($L\alpha_1$)	Gd($L\alpha_1$)	Sm($L\beta_{1,4}$)	Fe($K\alpha_1$)†	Dy($L\alpha_1$)	Ho($L\alpha_1$)	Pb($L\alpha_1$)	Th($L\alpha_1$)	U($L\alpha_1$)	Y($K\alpha_1$)
Chester	8	26.5	14	23.5	15.5	3.5	100+	14	22	6.5	74.5	2	8
Amelia	5	25	10	28.5	21.5	12.5	17	12	6	2	72.5	0	14.5
Arendal	6.5	26.5	21.5	33.5	27.5	12.5	24	14	13	4.5	44.5	3	36
Augusta	4.5	21	8.5	26	22.5	10.5	45	18.5	8.5	4.5	65	2.5	28.5
Madison	8	28.5	23	32	20.5	5	30	6.5	5.5	1.5	35.5	2.5	12
Minas Geraes	6	23.5	10.5	33	27.5	11.5	41.5	11.5	11.5	1.5	42.5	1	29
Missoula	5	27	10	35.5	24.5	13.5	30	9.5	8	6.5	58.5	1.5	4.5
S. Lynne	8	31	14.5	27.5	16.5	2.5	100+	7.5	1	1	29.5	.5	10
Toledo	8	30	13.5	30.5	20.5	5	46.5	10.5	5	2	39	2	34
Urals	8	32	14	31	19.5	4	30.5	7	4	1.5	38.5	0	19.5

* Norelco Spectrometer: Setting 8, 1.0, 8; 35 KV, 27 M.A.; Specimen size—120 mesh.

† Fe($K\alpha_1$) intensities include background estimated at 15.5 units.

mutual interferences precludes an attempt at this time to extend the semi-quantitative approach beyond this point.

Conclusions

Although the Chester monazite contains a considerable amount of intercrystalline goethite, it compares favorably with nine other monazite localities in physical, optical, differential thermal, and *x*-ray properties.

Monazite may be identified by its characteristic *x*-ray diffraction pattern. Dependable reflections are obtained and indexed. The range in individual (*hkl*) reflections among the ten specimens is shown, but does not yield any simple relation to chemical composition.

Differential thermal analysis indicates that the thermal pattern of pure monazite is featureless. The exothermic peaks obtained are considered to be caused by iron-bearing alteration minerals, and are sufficiently consistent to suggest the presence of monazite in thermal curves.

The nature of the alteration within monazite crystals is indicated by differential thermal analysis, *x*-ray fluorescence, and the use of the *x*-ray diffraction micro-camera. These point to an iron-bearing, non-hydrous, amorphous mineral or group of minerals capable of oxidation. Some form of concentration of the alteration products must be devised to continue this work.

Optical study of ten monazites does not provide a systematic relationship between index of refraction, 2V, birefringence, alteration, rare earth content, and thorium content. However, the influence of alteration on the cleavage is verified.

Qualitative chemical analysis of monazite may be accomplished by *x*-ray fluorescence. The method is adequate for the determination of relative amounts of rare earths among monazites, its sensitivity having been shown by the detection of predicted trends in rare earth content due to crystal fractionation. Accurate quantitative analysis is at present accomplished by emission spectroscopy of spectrophotometry. The extension of *x*-ray fluorescence to this field is anticipated by an analysis of the variables which now limit its use. As a step toward this end, a tabulation of the interferences encountered in the fluorescence analysis of monazite is included.

References

Arens, P. L. (1951), Differential thermal analysis of clays: Dissertation, Wageningen.

Blanchard, R. (1944), Chemical and mineralogical composition of twenty typical "limonites": *Am. Mineral.*, **29**, 111.

Dowling, P. H., Hendee, C. F., Kohler, T. R., and Parrish, W. (1956), Counters for *x*-ray analysis: *Philips Tech. Rev.*, **18**, No. 9, 262–275.

Dunn, H. W. (1955), A study of *x*-ray fluorescence for the analysis of rare earths and other complex groups: *Oak Ridge Nat. Lab., Rept.* No. *ORNL-1917* (Aug. 4, 1955).

Fankuchen, I., and Mark, H. (1944), *X*-ray studies of chain polymers: *Jour. App. Physics*, **15**, 367.

FINE, S., AND HENDEE, C. F. (1954), A table of x-ray K and L emission and critical absorption energies for all the elements: *Philips Tech. Rept.*, **86.**

VON GLISZCZYNSKI, S. (1939), Beitrag zur "isomorphie" von monazit und krokoit: *Zeit. Kr.*, **101,** 1–16.

GOLDSCHMIDT, V. M., AND THOMASSEN, L. (1924), Geochemische verteilungsgesetze der elemente III: *Videnskabsselskabet, Math. Naturv. Klasse, Skrifter.*, **5,** 7–58.

GRIM, R. E., AND ROWLAND, R. A. (1942), Differential thermal analysis of clay minerals and other hydrous materials: *Am. Mineral.*, **27,** 746–761, 801–818.

VON HEVESY, G. (1932), Chemical analysis by x-rays and its applications: McGraw-Hill Book Co., Inc., New York, 325 pp.

KELLEY, D. R., AND KERR, P. F. (1957), Clay alteration and ore, Temple Mountain, Utah: *Bull. Geol. Soc. Am.*, **68,** 1077–1100.

KERR, P. F., AND KULP, J. L. (1948), Multiple differential thermal analysis: *Am. Mineral.*, **33,** 387–419.

KLUG, H. P., AND ALEXANDER, L. E. (1954), X-ray diffraction procedures: John Wiley & Sons, Inc., New York, p. 36.

KULP, J. L., AND KERR, P. F. (1949), Improved differential thermal analysis apparatus: *Am. Mineral.*, **34,** 839–845.

KULP, J. L., AND PERFETTI, J. N. (1950), Thermal study of manganese oxides: *Mineral. Mag.*, **29,** 239–251.

KULP, J. L., AND TRITES, A. F. (1951), Differential thermal analysis of natural hydrous ferric oxides: *Am. Mineral.*, **36,** 23–44.

MACKENZIE, R. C. (1957), The differential thermal analysis of clays: *Mineral. Soc. London.*

MARKEWICZ, F. J., CHAO, E. C. T., AND MILTON, C. (1957), Radioactive minerals of New Jersey: *Program of Annual Meeting, Geol. Soc. Ann.*, p. 93.

MATTHEWS, W. D. (1894–95), Monazite and orthoclase from South Lyme, Conn.: *Sch. Mines Quart., Columbia Univ.*, **16,** 232.

MEYROWITZ, R., AND LARSEN, E. S., JR. (1951), Immersion liquids of high refractive index: *Am. Mineral.*, **36,** 746–750.

MILLER, D. C. (1957), Some considerations in the use of Pulse Height Analysis with x-rays: *Norelco Reporter, IV*, No. 2, 37–40.

MURATA, K. J., ROSE, H. J., JR., AND CARRON, M. K. (1953), Systematic variation of rare earths in monazite: *Geochim. et Cosmochim. Acta*, **4,** 292–300.

MURATA, K. J., ROSE, H. J., JR., CARRON, M. K., AND GLASS, J. J. (1957), Systematic variation of rare earth elements in cerium earth minerals: *Geochim. et Cosmochim. Acta*, **11,** 141–161.

PABST, A., AND HUTTON, C. O. (1951), Huttonite, a new monoclinic thorium silicate: *Am. Mineral.*, **36,** 60–69.

PARRISH, W. (1939), Unit cell and space group of monazite: *Am. Mineral.*, **24,** 651–652.

PARRISH, W. (1956), X-ray intensity measurements with counter tubes: *Philips Tech. Rev.*, **17,** 7–8, 206–221.

PARRISH, W., AND KOHLER, T. R. (1956), Use of counter tubes in x-ray analysis: *Rev. Sci. Inst.*, **27,** No. 10, 795–808.

POSNJACK, E., AND MERWIN, H. E. (1919), Hydrated ferric oxides: *Am. Jour. Sci.*, **47,** 311–348.

POWERS, M. C. (1957), X-ray fluorescent spectrometer conversion tables: Philips Electronics, Inc., New York.

SALMON, M. L., AND BLACKLEDGE, J. P. (1954), Analysis of rare earth mixtures by fluorescent x-ray spectroscopy: *Anal. Chem.*, **26,** 1667. Denver Univ., Denver Res. Inst., Progress in Research, 1–12.

Manuscript received August 15, 1958.